

# On Cooperative Coding for Narrowband PLC Networks

Lutz Lampe<sup>a</sup> and A.J. Han Vinck<sup>b</sup>

<sup>a</sup>*Department of Electrical and Computer Engineering, University of British Columbia, Vancouver, Canada*

<sup>b</sup>*Institute for Experimental Mathematics, University of Duisburg-Essen, Germany*

---

## Abstract

Low-frequency narrowband (LF NB) power line communications (PLC) is an old data-communication concept that has received renewed interest in industry, standardization, and academia for its potential to become an important element of the communication infrastructure supporting Smart Grid applications. In this paper, dedicated to Prof. Johannes Huber on the occasion of his 60th birthday, we review and discuss channel modeling and cooperative coding methods for LF NB PLC systems operating in low-voltage access networks.

*Keywords:* Power line communications (PLC), channel modeling, cooperative coding, bus systems.

---

## 1. Introduction

While the concept of data communication over power lines has been used for more than 100 years, it has only relatively recently returned to the centre stage of communication technologies that are subject of research and innovation. It started in the 1990s with broadband power line communications (PLC), operating from about 2 MHz to about 30 MHz or even beyond, and achieving data rates in excess of 100 Mbps [1, Ch. 7]. More recently, the focus has shifted towards low-frequency narrowband (LF NB) PLC systems, operating below 500 kHz and providing data rates of less than 500 kbps. Narrowband PLC for automation and control, for example in ripple control systems, has historically been the most popular form of PLC. However, with the arrival of the Smart Grid concept, and the potential of PLC to play a role in the blend of technologies composing the Smart Grid communications infrastructure, it has received renewed attention in research, development, and standardization [1, Sec. 8.2], [2].

LF NB PLC and its application in low-voltage (LV) power distribution grids in the access domain are the topic of this paper. It is dedicated to Prof. Johannes Huber, who has been a pioneer in the application of communication theory to PLC, on the occasion of his 60th birthday. In the first part of this paper (Sections 2 and 3), we present the application of two-conductor transmission line theory to produce and analyse the transfer functions for transmission over LV power lines in the access domain. This part may be seen as a tutorial summary of as well as a complementary view for a number of earlier works studying transfer characteristics for LF NB PLC such as

[3, 4, 5, 6, 7]. Considering idealized example scenarios in Section 3, we highlight the distance-dependent attenuation experienced in LF PLC networks. This leads us to the second part of this paper (Section 4), in which we discuss the use of repeaters to bridge larger distances in such PLC networks. In particular, considering PLC over transmission lines as a bus system, we present and compare different multihop transmission schemes. Following [8], we advocate the use of incremental redundancy, which we refer to as cooperative coding, to improve the achievable rate in PLC repeater systems. We also provide specific examples for cooperative coding schemes. This part of the paper is closely related to work on relay channels for wireless communications, in particular [9]. We believe that this relation is not coincidental, but emphasizes on the fact that many methods developed for wireless communications are applicable to PLC too.<sup>1</sup>

In closing this section, we hope that this paper provides an informative short course through channel-modeling and multihop-transmission concepts for LF NB PLC that will stimulate further research in this timely and relevant technology, especially in view of its application in Smart Grid implementations.

## 2. Transfer Functions in PLC Networks

The two-conductor transmission line formalism has often been used to model the power line channel and obtain transfer functions, cf. e.g. [4, 11], [1, Ch. 2]. While this formalism fails to capture all transmission modes of multi-conductor power line cables and mode coupling due to unsymmetries (cf. e.g. [12, 3, 13, 14] for more general modeling approaches

---

<sup>\*</sup>The work of L. Lampe was supported by the Alexander von Humboldt Foundation (while visiting the University of Duisburg-Essen) and the National Sciences and Engineering Research Council of Canada (NSERC).

*Email addresses:* Lampe@ece.ubc.ca (Lutz Lampe),  
vinck@iem.uni-due.de (A.J. Han Vinck)

---

<sup>1</sup>A prominent example is orthogonal frequency-division multiplexing (OFDM), whose application in PLC has early been advocated by Prof. Huber, in collaboration with iAd GmbH, cf. [10].

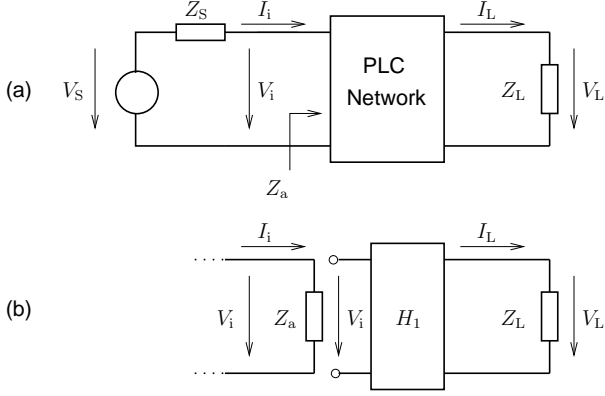


Figure 1: Loaded transmission line as (a) two-port network and (b) equivalent model.

based on multi-conductor transmission line theory) and necessitates idealized assumptions with regards to available topology and load information, it provides first analytical approximations and valuable insights in the transfer characteristics of PLC networks. The exposition below follows closely the concise description in [11, Sec. 3] and [1, Secs. 2.3 and 2.8].

Figure 1(a) shows the representation of a power line transmission system. The Helmholtz-Thévenin equivalent circuit of the transmitter is linked via a two-port circuit representing the PLC network to the load impedance modeling the receiver. The two-port network can be described by the transmission line parameters ( $ABCD$ -parameters) according to

$$\begin{bmatrix} V_i \\ I_i \end{bmatrix} = \begin{bmatrix} A & B \\ C & D \end{bmatrix} \begin{bmatrix} V_L \\ I_L \end{bmatrix}. \quad (1)$$

Given the  $ABCD$ -parameters, the relevant transfer functions relating input and load voltages are obtained as

$$H_1 \triangleq \frac{V_L}{V_i} = \frac{Z_L}{AZ_L + B} \quad (2)$$

$$H_2 \triangleq \frac{V_L}{V_s} = \frac{Z_L}{AZ_L + B + CZ_L Z_s + DZ_s}. \quad (3)$$

Furthermore, the access impedance follows as

$$Z_a = \frac{AZ_L + B}{CZ_L + D}. \quad (4)$$

The transfer function  $H_1$  and access impedance can be used for the equivalent transmission model in Figure 1(b), which is typically of interest for communications engineers. The magnitude transfer function  $|H_1|$  is often used to quantify “line losses”, while  $Z_a$  is responsible for “coupling losses” [5].

In order to obtain  $H_1$  or  $H_2$  and  $Z_a$ , the elements of the PLC network to which transmitter and receiver from the link of interest are connected, are modelled as transmission line pieces and shunt impedances, which are cascaded according to the network topology. The  $ABCD$ -parameters for a transmission line of length  $l$  are given by

$$\begin{aligned} A_{\text{line}} &= \cosh(\gamma l), & B_{\text{line}} &= Z_0 \sinh(\gamma l), \\ C_{\text{line}} &= \frac{1}{Z_0} \sinh(\gamma l), & D_{\text{line}} &= \cosh(\gamma l), \end{aligned} \quad (5)$$

where  $Z_0$  and  $\gamma$  denote the characteristic impedance and propagation constant of the cable, respectively. The parameters for a shunt with impedance  $Z_s$  are

$$A_{\text{sh}} = 1, \quad B_{\text{sh}} = 0, \quad C_{\text{sh}} = Z_s^{-1}, \quad D_{\text{sh}} = 1. \quad (6)$$

The parameters  $Z_0$ ,  $\gamma$ , and  $Z_s$  are generally frequency dependent, which renders the  $ABCD$ -parameters in (1) and thus the transfer functions  $H_1$  (2) and  $H_2$  (3) and the access impedance  $Z_a$  (4) depend on frequency  $f$ . For brevity, we omit explicit display of this dependency in the notation.

Characteristic impedance  $Z_0$  and propagation constant  $\gamma$  are commonly referred to as secondary cable parameters. They are related to the primary cable parameters  $R'$ ,  $G'$ ,  $L'$ , and  $C'$ , representing resistance, conductance, inductance, and capacitance per length, respectively, by

$$Z_0 = \sqrt{(R' + j2\pi fL')/(G' + j2\pi fC')} \quad (7)$$

and

$$\gamma = \sqrt{(R' + j2\pi fL')(G' + j2\pi fC')}. \quad (8)$$

The primary parameters depend on the physical cable characteristics as well as the signal coupling.

### 3. PLC Transmission Scenarios

We now put the formalism described in Section 2 to use to gain insight into the transmission characteristics over LV power lines in the access domain. To this end, we consider a number of scenarios for transmission between a transformer station and a house connection point. The scenarios are illustrated in Figures 2(a)-(e), and become more complex from top to bottom. In the first scenario in Figure 2(a) transmitter modem “Tx” and receiver modem “Rx” are connected by an unbranched power supply cable. This scenario is extended in Figure 2(b) by including the effect of the transformer impedance  $Z_T$  at Tx, using a transformer model presented and validated in [7], and the impedance  $Z_{\text{panel}}$  of the house connection point (“panel”) at Rx. For the numerical examples presented below we use NAYY150SE for the main supply cable and NAYY50SE for house connection cables (these are four-conductor power supply cables used for three-phase voltage supply in Europe, cf. e.g. [1, Fig. 2.16]). The scenario in Figure 2(b) corresponds to the transmission from a transformer station to the house connection point. In Figure 2(c) the reverse scenario is considered, i.e., transmission from the house to the transformer. The presence of additional branches, i.e., houses, on the main supply line is included in Figures 2(d) and (e).

#### 3.1. Parameters

To apply (2)-(4) for the transmission scenarios shown in Figures 2(a)-(e), we assume injection of the signal into two phases with the neutral conductor as return (see [1, Fig. 2.26]), for which the following approximations are derived in [15], [1, Sec. 2.3.3.1]:

$$\begin{aligned} R' &= \sqrt{\rho\pi f\mu_0/r^2}, & G' &= 2\pi fC' \tan(\delta_C), \\ L' &= \mu_0\vartheta/(2r), & C' &= 2\epsilon_0\epsilon_r\vartheta, \end{aligned} \quad (9)$$

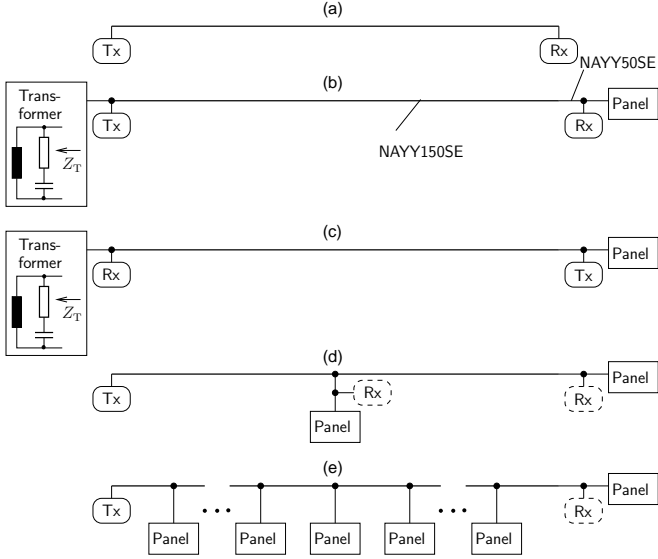


Figure 2: Illustration of simplified transmission scenarios.

where  $\mu_0$ ,  $\epsilon_0$ ,  $\epsilon_r$ ,  $\tan(\delta_C)$ , and  $\rho$  are the vacuum permeability and permittivity, relative permittivity and dielectric loss angle of the insulation, and specific resistance of the conductor, respectively, and  $r$  and  $\vartheta$  denote the radius of the cable and the thickness of the insulation (see [1, Fig. 2.26]). The numerical values for the NAYY150SE and NAYY50SE are  $r = 15.6$  mm,  $\vartheta = 3.6$  mm and  $r = 9.4$  mm,  $\vartheta = 2.8$  mm, respectively, and  $\epsilon_r = 4$  and  $\rho = 2.8 \cdot 10^{-8}$   $\Omega\text{m}$ , and we further assume  $\tan(\delta_C) = 0.01$ . The components of the transformer model (see Figure 2) are  $R_T = 8$   $\Omega$ ,  $L_T = 25$   $\mu\text{H}$ , and  $C_T = 48$  nF according to [7]. The length of the power supply cable NAYY150SE is chosen 1000 m. If not stated otherwise, the house connection cables NAYY50SE are assumed to be 20 m long (see Figure 2) and the impedance of the house connection point is chosen as  $Z_{\text{panel}} = 5$   $\Omega$  (the low impedance accounts for parallel indoor power lines branching off the house panel [1, Sec. 2.3.1]). Modem impedances are set to  $Z_S = Z_L = 50$   $\Omega$ . (As we mention later, the Tx impedance should be chosen smaller to reduce coupling losses.)

We hasten to point out that parameters like panel and modem impedances, cable types and lengths, etc. will vary notably for different LV networks and PLC implementations. Furthermore, panel impedances vary over time. But the results shown in the following for the specific parameter values given above allow us to draw some generally applicable conclusions to guide the design of (cooperative) PLC systems.

### 3.2. Numerical Results

Figures 3(a) and (b) show the magnitude transfer function  $|H_1|$  from (2) and  $|H_2|$  from (3) as function of frequency  $f$  in the range of 1 kHz to 500 kHz. Cases (a), (b), and (c) from Figure 2 are compared. Also included is the case of impedance matching at the receiver. For this case, we observe that power cable results in an attenuation that monotonically increases with frequency. However, attenuation is fairly moderate, e.g., only about 1.5 dB at 100 kHz for the 1 km of cable. The picture

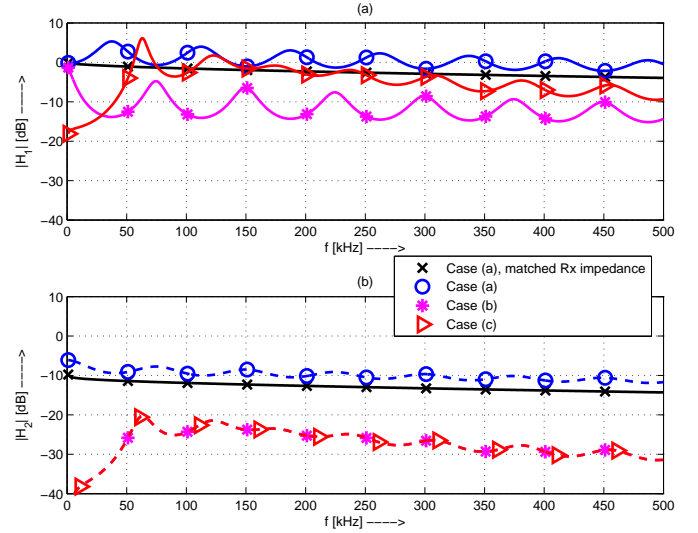


Figure 3: Magnitude transfer function as function of frequency  $f$  for scenarios from Figure 2. (a)  $|H_1|$  from (2), (b)  $|H_2|$  from (3).

changes when the Rx-impedance is not matched to the cable impedance. Let us first focus on  $|H_1|$  in Figure 3(a). As reflections occur on the line, the magnitude transfer function oscillates as function of frequency, overlaid by some small declining slope. Since the reflected wave travels the cable back and forth to arrive at Rx again, the extrema of the oscillations occur at  $\lambda/2 = 2$  km, where  $\lambda = 1/(\sqrt{\epsilon_0\epsilon_r\mu_0}f) = 1.5 \cdot 10^8/(f/\text{Hz})$  m. For case (b) the extrema are inverted compared to case (a), since the receiver-side impedance is small due to the low  $Z_{\text{panel}}$ , leading to a negative reflection coefficient. Furthermore, we observe much larger attenuation compared to case (a). This is caused by the low impedance of the house connection point being parallel to the Rx impedance, which clearly dominates the overall attenuation. Considering the reverse link, i.e., case (c) in Figure 2, emphasizes the role of the transformer impedance  $Z_T$ , which renders the total impedance on the receiver side frequency dependent. But attenuation is less pronounced than for case (b) with the low panel impedance parallel to Rx. Comparing  $|H_2|$  from (3) shown in Figure 3(b) to the curves in Figure 3(a) we note the significantly larger signal attenuation, which is due to the coupling losses included in the definition of  $|H_2|$ . These losses can be reduced (in principle to zero) by decreasing the Tx impedance [5]. It can be seen that the transfer function  $H_2$  is identical for cases (b) and (c), which demonstrates the channel symmetry [16].

Next, we move to more realistic cases with multiple branches along the power line. Figure 4 shows the magnitude transfer function  $|H_1|$  for case (d) in Figure 2. More specifically, Figure 4(a) shows the transfer function when the first house connection point is located at exactly the middle of the 1000 m supply cable, i.e., at 500 m. For Figure 4(b) an average over 100 magnitude transfer functions  $|H_1|$  is presented, for which the location of the first house connection point, the length of the house connection cables, and the panel impedances are generated randomly according to a uniform distribution over

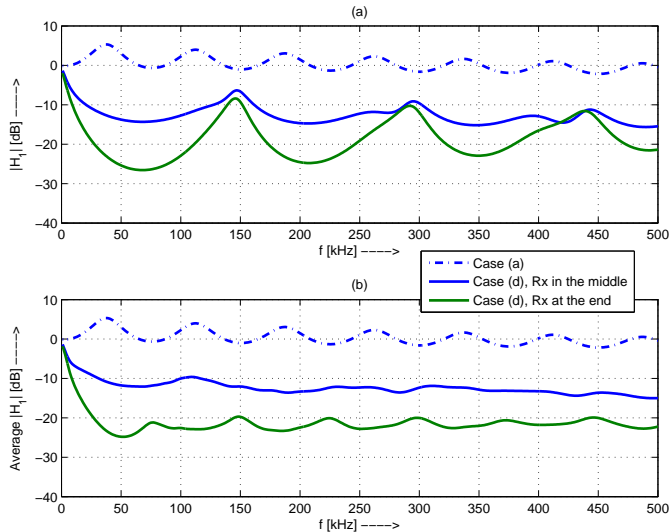


Figure 4: Magnitude transfer function as function of frequency  $f$  for Scenario (d) from Figure 2 with different locations of the receiver (Rx). Curve for Scenario (a) included as a reference. (a)  $|H_1|$  from (2), (b) average of  $|H_1|$  for 100 random line networks.

$[0, 1000]$  m,  $[0, 20]$  m, and  $[0, 5] \times j[-5, 5]$   $\Omega$ , respectively. We observe a significantly increased attenuation compared to the unbranched line (case (a) in Figure 2). In Figure 4(a), we note resonance effects, while the results in Figure 4(b) emphasize on the increase of attenuation with the overall transmission distance.

The latter effect becomes more pronounced for the case (e) in Figure 2 assuming 10 house connection points, whose transfer functions  $|H_1|$  at  $f = \{50, 100, 200, 300\}$  kHz are plotted in Figure 5. We observe that attenuation increases dramatically with distance between Tx and Rx for all frequencies. The range of attenuations is consistent with the 40-100 dB/km reported in [5, 4]. We would like to emphasize that the specific shape of the curves in Figure 5 strongly depends on the values of load impedances  $Z_{\text{panel}}$  and also the location of the house connection points. For example, loads with reactive components can lead to frequency dependencies due to resonance effects of loads [6], [1, Sec. 2.2.5].

#### 4. The PLC Channel as a Bus-System

Consistently with the literature, e.g. [5, 4], it has been established in the previous section that PLC users (i.e., customers) connected to the LV access network experience a signal attenuation which notably increases with the distance from the transmitter location. This means that in many cases a message needs to be transmitted via multiple hops from transmitter to repeater. Furthermore, since a transmitted signal may be overheard by multiple receivers due to the broadcast nature of the transmission line network, more sophisticated signal retransmission concepts, collectively referred to as cooperative communication, are applicable (cf. e.g. [17, 18, 19] for variants of cooperative communication in PLC).

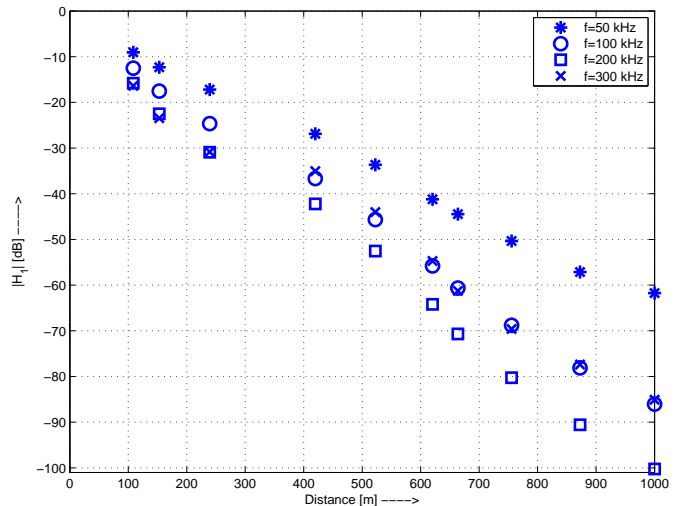


Figure 5: Magnitude transfer function  $|H_1|$  from (2) as function of distance from the transmitter Tx in scenario (e) from Figure 2 with 10 house connection points, at different frequencies  $f$ .

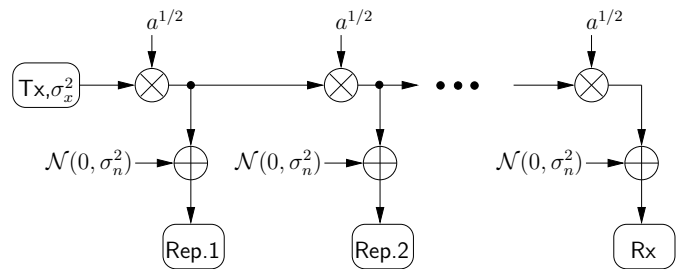


Figure 6: Model for transmission from Tx to Rx using repeaters. (Gain  $a^{1/2}$ , Tx power  $\sigma_x^2$ , AWGN power  $\sigma_n^2$ .)

In this work, we consider the transmission line as a bus system where only one transmitter can use the line to transmit information, and we study the concept of incremental redundancy using retransmissions, which we refer to as cooperative coding. We follow closely the initial work presented in [8].

##### 4.1. Transmission Model

Motivated by the results presented in Section 3.2, we apply the simplified transmission model shown in Figure 6. The transmitter Tx wishes communicate to a destination Rx at distance  $D$  and may make use of  $N - 1$  repeaters  $i, i = 1, \dots, N - 1$ . The (Tx/repeater)-to-(repeater/Rx) distance is  $d = D/N$ . Each link of distance  $d$  is associated with an attenuation factor  $(a(d))^{1/2}$  (see Figure 5). Furthermore, we assume disturbance by additive white Gaussian noise (AWGN) with equal variance. We are aware that AWGN is a fairly simplistic representation for the rich noise environment experienced in PLC (cf. e.g. [1, Ch. 2]), but it shall suffice here for the introduction of cooperative coding. Future extensions will replace the AWGN by mixture noise models, perhaps with memory [20], to account for the effects of impulse noise seen in PLC channels [21].

#### 4.2. Communication Strategies

Suppose that the transmitter Tx sends a binary signal and at each receiver a hard decision is made. Then, each connection can be described as a binary symmetric channel with a crossover probability, i.e., error probability  $P_e$ , determined by the receiver-side signal-to-noise power ratio (SNR)  $\gamma$  through

$$P_e = Q(\sqrt{c \cdot \gamma}), \quad (10)$$

where  $Q(\cdot)$  is the Gaussian-Q function, and  $c$  is a constant depending on the modulation scheme. For a link of distance  $d$  we have  $\gamma = a(d)\sigma_x^2/\sigma_n^2$ . In the following, we discuss possible communication strategies to efficiently use and operate repeaters. The first two strategies fall into the category of conventional multihop, while the third makes use of incremental redundancy. All three schemes have in common that source and repeaters transmit the message only in one out of  $N$  time slots; the use of spatial reuse, which is not discussed here, may enable further data rate improvements.

**Detect-and-forward:** In the connection between the transmitter Tx and receiver Rx, the intermediate receivers can act as detect-and-forward repeaters. After taking a hard decision on the received signal, repeater  $i$  sends the remodulated signal to receiver  $i + 1$ . If at the first repeater the detection error probability is  $P_e$ , then the error probability at the  $N$ th receiver is given by  $1 - \sum_{i=0}^{\lfloor N/2 \rfloor} \binom{N}{2i} P_e^{2i} (1 - P_e)^{N-2i} \approx NP_e$ . While this linear increase of error probability with distance is far better than the exponential growth experienced without repeaters, the use of repetitions reduces the overall transmission efficiency by a factor of  $N$ . Since  $\gamma$  and thus  $P_e$  is determined by the attenuation factor  $a(d)$ , and  $d = D/N$ , the number and location of repeaters could be optimized such that  $N$  is minimized subject to an upper bound on the error rate  $NP_e$  at the destination.

**Decode-and-forward:** As in point-to-point connections, we can also use coding to improve the communication efficiency. Given the model described above, we have the capacity  $C(d) = 1 - e_2(P_e)$  for a link of distance  $d$ , where  $e_2(\cdot)$  is the binary entropy function. Assuming that  $C(d)$  is a measure for the achievable rate with coding, which is monotonically decreasing with increasing  $d$ , and considering that  $N$  hops reduce the overall available rate to

$$C_{df} = C(d)/N, \quad (11)$$

we again have an optimization problem for the number and thus location of repeaters.

**Cooperative Coding:** Since we have a bus structure, we can use the fact that all users connected to the bus are able to hear the communication. The achievable rate for communication between transmitter Tx and the first receiver is  $k/n_1 = C(d)$ , i.e., after  $n_1$  transmissions the first receiver can decode the transmitted  $k$  bits of information. Simultaneously, the amount of information received at the second receiver is  $n_1 C(2d)$ . To assist the second receiver in decoding the transmitted message, repeater 1 sends  $n_2$  encoded symbols, such that  $k = n_1 C(2d) + n_2 C(d)$ . For the third transmission, repeater 2 transmits  $n_3$  encoded symbols such that  $k = n_1 C(3d) + n_2 C(2d) + n_3 C(d)$  and the third receiver

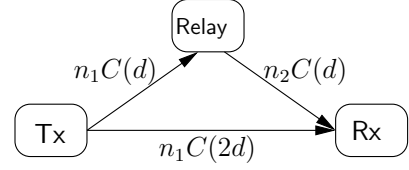


Figure 7: The bus system with two links seen as a relay channel.

can decode the message. For the destination, we have

$$k = \sum_{i=1}^N n_i C((N - i + 1)d). \quad (12)$$

In summary, given  $k$  and the link capacities  $C(id)$ ,  $i = 1, \dots, N$ , the lengths  $n_i$ ,  $i = 1, \dots, N$ , are obtained from

$$\begin{bmatrix} C(d) & 0 & \dots \\ C(2d) & C(d) & 0 & \dots \\ \vdots & \vdots & \vdots & \vdots \\ C(Nd) & C((N-1)d) & \dots & C(d) \end{bmatrix} \begin{bmatrix} n_1 \\ n_2 \\ \vdots \\ n_N \end{bmatrix} = \begin{bmatrix} k \\ k \\ \vdots \\ k \end{bmatrix} \quad (13)$$

and the overall achievable rate is

$$C_{coop} = k / \sum_{i=1}^N n_i. \quad (14)$$

If we do not use the cooperative coding, we have the rate from (11)  $C_{df} = k/(Nn_1)$ .

As an example, let us consider  $N = 2$ . With decode-and-forward the rate is  $C_{df} = \frac{1}{2}C(d) = k/(2n_1)$ . With cooperative coding we obtain

$$C_{coop} = \frac{k}{n_1 + n_2} = \frac{C(d)}{2 - C(2d)/C(d)} > \frac{1}{2}C(d). \quad (15)$$

Clearly, if  $a = 1$ , then  $C(2d) = C(d)$  and thus  $n_2 = 0$  and the repeater is not used. However, for  $a < 1$ ,  $C(2d) < C(d)$ , and cooperative coding has an advantage. If, for example,  $P_e = 10^{-3}$  and  $a = -10$  dB, then  $C(d) = 0.99$  bit/transmission and  $C(2d) = 0.36$  bit/transmission. Hence, cooperative coding increases the rate from 0.36 bit/transmission using no repetition or 0.49 bit/transmission using decode-and-forward to  $C(d)/(2 - C(2d)/C(d)) = 0.60$  bit/transmission.

The concepts of detect/decode-and-forward and cooperative coding are of course not new, but have been studied for wireless communications using relays, cf. e.g. [22], where the focus is on diversity, i.e., mitigating the effects of fading. Figure 7 illustrates the bus system for  $N = 2$  as a relay link, using Protocol II from [22, Table I]. The use of incremental redundancy in cooperative coding as described above has also been considered as a generalization of hybrid automatic repeat-request (ARQ) for wireless relay networks in [9]. Furthermore, [23, 24] study the use of rateless codes to accomplish code combining (a.k.a. information combining) for relay transmission.

To outline the advantages of cooperative coding, consider a binary modulation scheme ( $c = 2$  in (10)) with a transmitter-side SNR of  $\gamma_{Tx} = \sigma_x^2/\sigma_n^2 = 13$  dB, and a Tx-Rx-distance of

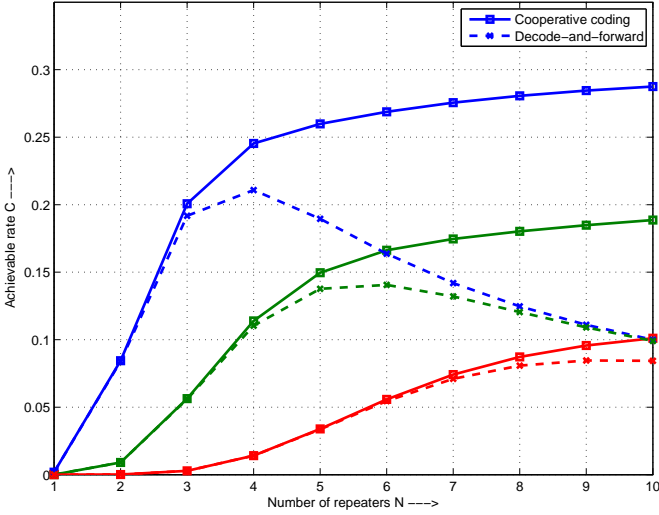


Figure 8: Achievable rate for cooperative coding  $C_{\text{coop}}$  and decode-and-forward  $C_{\text{df}}$  as function of number of repeaters  $N$ . Link of 1 km and attenuation of  $\{40, 60, 100\}$  dB/km (curves from top to bottom).

$D = 1$  km. The attenuation for a link of length  $d = D/N$  is given by  $a = 10^{-\delta d}$ , where we choose  $\delta \in \{40, 60, 100\}$  dB/km (cf. Figure 5 and [5, 4]). The error probability for direct transmission over  $i$  links follows from (10) as  $P_e^{(i)} = Q(\sqrt{2a^i \gamma_{\text{Tx}}})$ , and the corresponding link capacity as  $C(i \cdot d) = 1 - e_2(P_e^{(i)})$ . We then can compute the achievable data rate for decode-and-forward and cooperative coding from (11) and (14), respectively. Figure 8 shows the achievable rate as function of the number of repeaters  $N$ . We observe that cooperative coding achieves a higher rate for a given number of repeaters. In particular, conventional multihop reaches a maximum rate at a certain repeater distance  $d = D/N$ , which decreases when repeater distance decreases through the addition of repeaters. Cooperative decoding, however, experiences a continuing increase in achievable rate for increasing  $N$  and thus decreasing repeater distance  $d$ .

#### 4.3. Example for Cooperative Coding

We use the  $(7, 4)$  Hamming code to illustrate an implementation of cooperative coding with a fixed-rate code. Suppose that we have a bus with only  $N = 2$  links. The length of the links is such that we expect a single error in a received code word per link. For the transmission using two links in tandem via detect-and-forward we expect two errors to occur, which cannot always be corrected. Applying decode-and-forward would allow error free transmission. But in both cases, the rate is only  $4/14$  bits per transmission. For cooperative coding, we use the Hamming code generated by the encoding matrix

$$G = \begin{bmatrix} 1 & 0 & 0 & 1 & 1 & 0 & 0 \\ 0 & 1 & 0 & 1 & 0 & 1 & 0 \\ 0 & 0 & 1 & 0 & 1 & 1 & 0 \\ 1 & 1 & 1 & 1 & 1 & 1 & 1 \end{bmatrix} \quad (16)$$

The reason for this choice of encoding matrix will be made clear in the following. The first receiver can decode the code word

if it has no more than a single error. The second receiver also receives a signal, but it cannot reliably decode the transmitted code word. The first receiver (repeater), after decoding, encodes the first three information bits with a minimum-distance-3 shortened Hamming code of length 6, generated by the code words  $[100110]$ ,  $[010101]$ ,  $[001011]$  (see (16)). The second receiver can decode the received code word, since it contains no more than a single error. After decoding, the second receiver can subtract the code word connected to these three information bits from the first reception and decodes the fourth information bit using the minimum distance 7 code generated by  $[1111111]$  which is able to correct three errors. The overall efficiency is  $4/(7 + 6) > 4/14$ . The example shows the importance of the code generator representation. Following this strategy, [25] defined the optimum distance profile (ODP) of linear block codes. Using the ODP, for particular codes, we are able to specify the maximum minimum distance of a sub-code. The ODP depends on the initial encoding matrix, as in the example.

The extension to Reed Solomon (RS) codes can be explained using the  $k/n$  RS-encoder matrix

$$G = \begin{bmatrix} 1 & 1 & 1 & \dots & 1 \\ 1 & \alpha & \alpha^2 & \dots & \alpha^{n-1} \\ 1 & \alpha^2 & \alpha^4 & \dots & \alpha^{2(n-1)} \\ \vdots & & & & \\ 1 & \alpha^{k-1} & \alpha^{2(k-1)} & \dots & \alpha^{(k-1)(n-1)} \end{bmatrix}, \quad (17)$$

where the  $\alpha$  is a primitive element from the  $\text{GF}(2^m)$  and  $n \leq 2^m - 1$ . Suppose again that  $N = 2$  and that we start with the  $k \times n$  encoding matrix  $G$  at Tx. The repeater has an encoder matrix generating the  $(n_1, k_1)$ -RS code consisting of the top  $k_1$  rows of length  $n_1$  of  $G$ , where  $n_1 < n$ . Tx encodes  $k$  symbols and forwards the code word to the repeater. The repeater can decode the received word from Tx, whereas Rx can listen but not decode since the reception is too noisy. The repeater then encodes the first  $k_1$  symbols to Rx using the  $(n_1, k_1)$ -RS code. Rx is assumed to be able to decode these  $k_1$  symbols and subtracts the influence from the first received code word. Since the minimum distance of the remaining code is increased, Rx can decode the whole code word. The performance of this method depends on the knowledge of the respective channel parameters and can be optimized for particular values of the channel parameters. To be specific, consider Figure 7 and assume that the fraction of symbols errors in the link from Tx to Relay and from Relay to Rx is  $p$ , leading to a redundancy of  $2pn$  symbols for codewords of length  $n$ . The fraction of symbol errors to be corrected in the direct link between Tx and Rx is  $\eta p$ , where  $\eta > 1$ . If these errors have to be corrected, the RS code has redundancy  $2\eta pn$  symbols. Hence, assuming  $\eta p < 1/2$ , we can express the throughputs for the different strategies as follows:

$$R_{\text{Tx} \rightarrow \text{Rx}} = \frac{k}{n} = 1 - 2\eta p, \quad (18)$$

$$R_{\text{Tx} \rightarrow \text{Relay} \rightarrow \text{Rx}} = \frac{k}{2n} = \frac{1 - 2p}{2}, \quad (19)$$

$$R_{\text{coop}} = \frac{k}{n + n_1} = \frac{(1 - 2p)^2}{1 + 2\eta p - 4p}. \quad (20)$$

Comparing these rates, we conclude that  $R_{\text{coop}} > R_{\text{Tx} \rightarrow \text{Rx}}$  for all  $\eta > 1$  and  $R_{\text{coop}} > R_{\text{Tx} \rightarrow \text{Relay} \rightarrow \text{Rx}}$  for  $\eta < 1/(2p)$ .

It is easy to extend this strategy to more than  $N = 2$  links, using the approach that leads to (13). Furthermore, we note that a similar idea was used by Dorsch [26], and later analyzed by Huber [27], for incremental-redundancy ARQ using RS codes. Finally, while it is convenient to apply punctured subcodes of the starting code at repeaters for the described communication strategy, which is easy to do for RS codes, since the punctured subcodes are again (by definition) RS codes, it is not necessary to use a chain of subcodes. The use of codes with the specified number of information symbols and minimum distance would suffice.

## 5. Conclusion

In this paper, we have studied transfer function characteristics for LF NB PLC networks operating in the access domain. Exemplary numerical results have shown that PLC signals undergo significant distance-dependent attenuation, which makes multihop transmission using repeaters mandatory. Considering such multihop PLC as a bus system, we have demonstrated the benefits in terms of achievable data rate that derive from the application of cooperative coding, a concept that has intensely been discussed in wireless communications over the past 10 years.

## References

- [1] H. Ferreira, L. Lampe, J. Newbury, T. Swart (Editors), *Power Line Communications*, John Wiley & Sons, 2010.
- [2] S. Galli, A. Scaglione, Z. Wang, For the grid and through the grid: The role of power line communications in the Smart Grid, Proc. IEEE Accepted for publication.
- [3] M. Karl, K. Dostert, Übertragungseigenschaften des Niederspannungs-Energieversorgungsnetzes zur digitalen Datenübertragung im Frequenzbereich von 10 kHz bis 150 kHz, in: *Kleinheubacher Berichte*, Vol. 39, 1995, pp. 333–342, (in German).
- [4] O. Hooijen, On the relation between network-topology and power line signal attenuation, in: *Intl. Symp. Power Line Commun. and its Appl.*, Tokyo, Japan, 1998, pp. 45–55.
- [5] O. Hooijen, A channel model for the residential power circuit used as a digital communications medium, *IEEE Trans. Electromagn. Compat.* 40 (4) (1998) 331–336.
- [6] H. Philipps, Modelling of powerline communication channels, in: *Intl. Symp. Power Line Commun. and its Appl.*, Lancaster, UK, 1999, pp. 14–21.
- [7] K. Dostert, M. Zimmermann, T. Waldeck, M. Arzberger, Fundamental properties of the low-voltage power distribution grid used as a data channel, *European Transactions on Telecommunications* 21 (3) (2000) 297–306.
- [8] V. Balakirsky, A. Vinck, Potential performance of PLC systems composed of several communication links, in: *Intl. Symp. Power Line Commun. and its Appl.*, Vancouver, 2005, pp. 12–16.
- [9] B. Zhao, M. Valenti, Practical relay networks: A generalization of hybrid-ARQ, *IEEE J. Select. Areas Commun.* 23 (1) (2005) 7–18.
- [10] T. Wagner, Untersuchung eines DMT-bertragsverfahrens und dessen Implementierung mit Hilfe eines Signalprozessors, Diplomarbeit am Lehrstuhl für Nachrichtentechnik, FAU Erlangen-Nürnberg, (in German) (Aug. 1996).
- [11] T. Esmailian, F. Kschischang, P. Gulak, In-building power lines as high-speed communication channels: Channel characterization and a test channel ensemble, *International Journal of Communication Systems* 16 (2003) 381–400.
- [12] M. Hardy, S. Ardalan, J. O’Neal, Jr., L. Gale, K. Shuey, A model for communication signal propagation on three phase power distribution lines, *IEEE Trans. Power Delivery* 6 (1991) 966–972.
- [13] T. Banwell, S. Galli, A Novel Approach to Modeling of the Indoor Power Line Channel — Part I: Circuit Analysis and Companion Model, *IEEE Trans. Power Delivery* 20 (2005) 655–663.
- [14] T. Sartenaer, P. Delogne, Deterministic modeling of the (shielded) outdoor power line channel based on the multiconductor transmission line equations, *IEEE J. Select. Areas Commun.* 24 (2006) 1277–1291.
- [15] T. Waldeck, M. Zimmermann, K. Dostert, Hochratige Datenübertragung auf elektrischen Energieverteilnetzen im Frequenzbereich bis 20 MHz, Tech. rep., University of Karlsruhe, (in German) (Dec. 1996).
- [16] T. Banwell, S. Galli, On the symmetry of the power line channel, in: *Intl. Symp. Power Line Commun. and its Appl.*, Malmö, Sweden, 2001.
- [17] L. Lampe, R. Schober, S. Yiu, Distributed space-time block coding for multihop transmission in power line communication networks, *IEEE J. Select. Areas Commun.* 24 (2006) 1389–1400.
- [18] G. Bumiller, L. Lampe, H. Hrasnica, Power line communications for large-scale control and automation systems, *IEEE Commun. Mag.* 48 (4) (2010) 106–113.
- [19] G. Bumiller, *Single Frequency Network Technology for Fast ad hoc Communication Networks over Power Lines*, WiKu-Wissenschaftsverlag Dr. Stein, 2010.
- [20] J. Mitra, L. Lampe, Convolutionally coded transmission over Markov-Gaussian channels: Analysis and decoding metrics, *IEEE Trans. Commun.* 58 (7) (2010) 1939–1949.
- [21] M. Zimmermann, K. Dostert, Analysis and modeling of impulsive noise in broadband powerline communications, *IEEE Trans. Electromagn. Compat.* 44 (1) (2002) 249–258.
- [22] R. Nabar, H. Bölcskei, F. Kneubühler, Fading relay channels: Performance limits and space-time signal design, *IEEE J. Select. Areas Commun.* 22 (2004) 1099–1109.
- [23] A. Molisch, N. Mehta, J. Yedidia, J. Zhang, Performance of fountain codes in collaborative relay networks, *IEEE Trans. Wireless Commun.* 6 (11) (2007) 4108 – 4119.
- [24] A. Ravanshid, L. Lampe, J. Huber, Dynamic decode-and-forward relaying using raptor codes, in revision: *IEEE Trans. Wirel. Commun.*
- [25] Y. Luo, A. H. Vinck, Y. Chen, On the optimum distance profile about linear block code, *IEEE Trans. Inform. Theory* 56 (2010) 1007–1014.
- [26] B. Dorsch, Successive check digits rather than information repetition, in: *IEE Int. Conf. Comm. (ICC)*, Boston, MA, USA, 1983, pp. 323–327.
- [27] J. Huber, On the performance of a hybrid coding scheme, in: *Intern. Zurich Seminar*, Zürich, Switzerland, 1984.